Excited State Properties of Quinoxaline-Substituted Platinum 1,2-Enedithiolates

Sharada P. Kaiwar, Anthony Vodacek, Neil V. Blough,* and Robert S. Pilato*

Contribution from the Department of Chemistry and Biochemistry, The University of Maryland, College Park, Maryland 20742

Received August 2, 1996. Revised Manuscript Received December 11, 1996[⊗]

Abstract: The complexes (dppe)M{S_2C_2(2-quinoxaline)(R)}, where dppe = (diphenylphosphino)ethane, M = Ni, Pd, and Pt, and R = H and Me, have as their lowest-energy band an intraligand charge transfer transition (ILCT). Excitation of deaerated solutions of (dppe)Pt{S_2C_2(2-quinoxaline)(R)} lead to emissions from an ^{1}ILCT* and an ^{3}ILCT*. The lifetimes of these excited states (τ) and the quantum yields for the emissions (ϕ) for (dppe)Pt{S_2C_2(2-quinoxaline)(H)} in CH_3CN are $^1\tau = 0.16$ ns,$^1\phi = 0.005$ and $^3\tau = 3.3$ μs, $^3\phi = 0.01$, respectively. The ^{3}ILCT* of these quinoxaline-substituted complexes can undergo a diverse suite of excited state reactions, including electron, proton, and hydrogen atom transfers. The second order rate constants (k_q) for the quenching of the ^{3}ILCT* emission by acids increases with the thermodynamic driving force for the excited state proton transfer, an observation consistent with excited state electron and hydrogen atom transfers. Dihydroquinone and *p*-methoxyphenol are substantially better quenching agents than excited state proton transfer would predict and thermodynamic calculations suggest that they quench the ^{3}ILCT* by hydrogen atom transfer.

Introduction

Luminescent transition metal complexes have been employed successfully in the study of long-range electron transfer[1−5] and the tagging and cutting of DNA.[6−12] These complexes may also prove useful as catalysts in the conversion of light to chemical energy and as chemical sensors.[13−15] Most of the work on luminescent metal complexes has focused on the photophysical and photochemical properties of polypyridyl complexes, particularly those of ruthenium.[16] More recently, the 1,2-enedithiolate and 1,1-dithiolate complexes of platinum have emerged as an interesting and potentially important new class of room temperature solution lumiphores.[17−23] In most of these complexes, light emission is thought to arise from either a metal to ligand charge transfer transition (MLCT) or an interligand charge transfer transition (LLCT). The interligand band is thought to result from a dithiolate → ancillary ligand π^* transition.[17,23] This transition requires that the metal complex contains an ancillary ligand (such as diimino or polypyridyl) with low-lying π^* orbitals.

The work presented here provides the first description of the photophysical and photochemical properties of a new family of heterocyclic-substituted platinum-1,2-enedithiolate complexes, (dppe)Pt{S_2C_2(heterocycle)(R)}, where dppe = (diphenylphosphino)ethane (see Scheme 1). A new method was developed to prepare these complexes, and although a wide range of heterocyclic groups can be incorporated,[24] this report is limited to those complexes where the heterocycle is a quinoxaline. These complexes exhibit luminescence in solution at room temperature via both the singlet and triplet excited states of an intraligand charge transfer transition (ILCT), best described as a 1,2-enedithiolate π → heterocycle π^*.

This excited state localizes additional electron density on the heterocycle, and hence, the excited state is more basic than the ground state. Quenching of the long-lived ^{3}ILCT* excited state with a range of organic acids has provided experimental evidence that, like electron transfer, the rate of excited state proton transfer is governed by the thermodynamic driving force

[⊗] Abstract published in *Advance ACS Abstracts,* March 15, 1997.

(1) (a) Winkler, J. R.; Gray, H. B. *Chem. Rev.* **1992**, *92*, 369−79. (b) Isied, S. S.; Ogawa, M. Y.; Wishart, J. F. *Chem. Rev.* **1992**, *92*, 381−94

(2) Nocera, D. G.; Winkler, J. R.; Yocom, K. M.; Bordignon, E.; Gray, H. B. *J. Am. Chem. Soc.* **1984**, *106*, 5145−50.

(3) Lieber, C. M.; Karas, J. L.; Gray, H. B. *J. Am. Chem. Soc.* **1987**, *109*, 3778−9.

(4) Beratan, D. N.; Onuchic, J. N.; Betts, J. N.; Bowler, B. E.; Gray, H. B. *J. Am. Chem. Soc.* **1990**, *112*, 7915−21.

(5) Chang, I.-J.; Gray, H. B.; Winkler, J. R. *J. Am. Chem. Soc.* **1991**, *113*, 7056−57.

(6) Arena, G.; Scolaro, L. M.; Pasternack, R. F.; Romeo, R. *Inorg. Chem.* **1995**, *34*, 2994−3002.

(7) Friedman, A. E.; Chambron, J. C.; Sauvage, J. P.; Turro, N. J.; Barton, J. K. *J. Am. Chem. Soc.* **1990**, *112*, 4960−2.

(8) Farrell, N.; Appleton, T. G.; Qu, Y.; Roberts, J. D.; Suares Fontes, A. P.; Skov, K. A.; Wu, P.; Zou, Y. *Biochemistry* **1995**, *34*, 15480−86.

(9) (a) Friedman, A. E.; Chambron, J.-C.; Sauvage, J.-P.; Turro, N. J.; Barton, J. K. *J. Am. Chem. Soc.* **1990**, *112*, 4960−2. (b) Hall, D. B.; Holmlin, R. D.; Barton, J. K. *Nature* **1996**, *382*, 731. (c) Arkin, M. R.; Stemp, E. D. A.; Holmlin, R. E.; Barton, J. K.; Hörmann, A.; Olson, E. J. C.; Barbara, P. F. *Science* **1996**, *273,* 475.

(10) Pyle, A. M.; Rehmann, J. P.; Meshoyrer, R.; Kumar, C. V.; Turro, N. J.; Barton, J. K. *J. Am. Chem. Soc.* **1989**, *111*, 3051−8.

(11) Liu, H.-Q.; Peng, S.-M.; Che, C. M. *J. Chem. Soc., Chem. Commun.* **1995**, 509−10.

(12) Breiner, K. M.; Daugherty, M. A.; Oas, T. G.; Thorp, H. H. *J. Am. Chem. Soc.* **1995**, *117*, 11673−79.

(13) (a) Liang, P.; Dong, L.; Martin, M. T. *J. Am. Chem. Soc.* **1996**, *118*, 9198−9. (b) Blackburn, G. G.; Shah, H. P.; Kenten, J. H.; Leland, J.; Kamin, R. K.; Wilkins, E.; Wu, T.-T.; Massey, R. J. *Clim. Chem.* **1991**, *37*, 1534−39.

(14) (a) Sykora, J.; Sima, J. *Coord. Chem. Rev.* **1990**, *107*, 1−192. (b) Ledney, M. I.; Dutta, P. K. *J. Am. Chem. Soc.* **1995**, *117*, 7687−95.

(15) Sabatani, E.; Nikol, H. D.; Gray, H. B.; Anson, F. C. *J. Am. Chem. Soc.* **1996**, *118*, 1158−63.

(16) Juris, A.; Balzani, V.; Barigelletti, F.; Campagna, S.; Belser, P.; Von Zelewsky, A. *Coord. Chem. Rev.* **1988**, *84*, 85−277.

(17) Cummings, S. D.; Eisenberg, R. *J. Am. Chem. Soc.* **1996**, *118*, 1949−60.

(18) Cummings, D. S.; Eisenberg, R. *Inorg. Chem.* **1995**, *34*, 2007−14.

(19) Cummings, D. S.; Eisenberg, R. *Inorg. Chem.* **1995**, *34*, 3396−403.

(20) Bevilacqua, M. J.; Eisenberg, R. *Inorg. Chem.* **1994**, *33*, 2913−23.

(21) Bevilacqua, J. M.; Zuleta, J. A.; Eisenberg, R. *Inorg. Chem.* **1993**, *32*, 3689−93.

(22) Zuleta, J. A.; Bevilacqua, J. M.; Eisenberg, R. *Coord. Chem. Rev.* **1991**, *111*, 237−48.

(23) Zuleta, J. A.; Bevilacqua, J. M.; Proserpio, D. M.; Harvey, P. D.; Eisenberg, R. *Inorg. Chem.* **1992**, *31*, 2396−404.

(24) (a) Hsu, J.; Bonangolino, C.; Kaiwar, S. P.; Boggs, C.; Fettinger, J.; Rheingold, A. L.; Pilato, R. S. *Inorg. Chem.* **1996**, *35*, 4743−4751. (b) Manuscript in preparation.

S0002-7863(96)02699-6 CCC: $14.00

Scheme 1

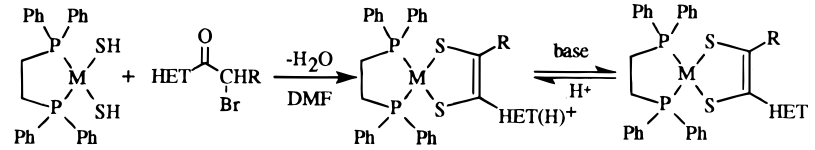

M	HET (R)	M		
Ni **1**	2-quin (H)	Ni, Pd, Pt	**4**, **5**,**6**	**8**, **9**,**10**	47, 52, 43 %
Pd **2**	2-quin (Me)	Pt	**7**	**11**	49 %
Pt **3**					

for the reaction. This relationship made it possible to distinguish the excited state proton transfer reactions of these complexes from the excited state hydrogen atom transfer reactions.

Experimental Section

Materials. The (dppe)M{S_2C_2(heterocycle)(R)} species (where M = Ni, Pd, and Pt and dppe = (diphenylphosphino)ethane, heterocycle = quinoxaline or quinoxalinium and R = H or Me) were prepared according to the literature procedures.[24] All reactions were performed under an atmosphere of nitrogen using standard Schlenk line techniques. Workups were performed in air unless stated otherwise. Dichloromethane, acetonitrile, and pentane were dried over calcium hydride and distilled under nitrogen. Diethyl ether, tetrahydrofuran, and dioxane were dried over sodium/benzophenone and distilled under nitrogen. Triethylamine was dried over potassium hydroxide and vacuum distilled. Phenol, 4-methoxyphenol, *o*-nitrophenol, 1,3-diaminopropane, benzoic acid, salicylic acid, pyridine, 1,4-dihydroquinone, 1,2-dinitrobenzene (DNB), dicyanobenzene (DCB), *N*,*N*-dimethylaniline (DMA), and *N*,*N*,*N*′,*N*′-tetramethyl-*p*-phenylenediamine (NTMP) were purchased from either Acros or Aldrich Chemical and were used without further purification. The tetraphenylborate salts of pyridinium, triethylammonium, and 1,3-diammoniopropane were prepared from the chloride salts in water by the addition of excess sodium tetraphenylborate. The insoluble tetraphenylborate salts were collected by filtration and dried under vacuo.

Physical Measurements. UV-vis spectra were recorded on either a Perkin Elmer Lambda 2S or a Hewlet Packard 8452A spectrometer. FAB mass spectral data were collected on a Magnetic Sector VG 7070E.

Luminescence Measurements. Room temperature excitation and emission spectra were acquired with a SLM AB2 fluorescence spectrometer. Emission spectra were corrected for instrumental response using factors supplied by the manufacturer. Oxygen-free luminescence measurements were made on 10^{-5} M solutions of **10** and **11** (see Scheme 1) that were deoxygenated by three freeze−pump−thaw N_2-backfill cycles in a fluorescence cell equipped with a reservoir and a Teflon valve.

Quantum yields, ϕ, were calculated relative to Zn(tpp){$\phi = 0.04$}[25] (tpp = tetraphenylporphyrin), in air and under Ar, from the areas of the instrument-corrected emission spectra. The quantum yield for the lower-energy emission band, $^3\phi$, was estimated from the difference in the emission areas of argon- and O_2-saturated solutions of **10** and **11**. In O_2-saturated solutions, little if any emission from the lower-energy band was observed. Because the higher-energy emission band was unaffected by these conditions, the quantum yield for the higher-energy emission band, $^1\phi$, was obtained directly from the emission areas of O_2-saturated solutions of **10** and **11**.

Lifetime measurements for **10** and **11** were determined with an ISS K2 digital frequency−domain spectrofluorometer. The excitation source was a 300 W Xenon lamp, and the bandpass of the excitation monochromator was 16 nm. Sample and reference solutions were contained in 1 cm quartz cells at room temperature. A scattering solution of glycogen in Milli-Q water was used as the reference. For some low-intensity samples, a neutral density filter was used to reduce the intensity of the reference scatter. Single channel detection at 90° was employed, with longpass filters used to block the excitation line and Raman scatter from the sample. Lifetimes were determined from the frequency dependence of the signal phase shifts and demodulation, relative to the reference, using the ISS least squares analysis software. The minimization procedure assumed discrete lifetimes. The procedure provided lifetimes, fractional photon contributions, and χ^2 for the least squares fit.

Triplet Quenching Experiments. Second-order rate constants for the quenching of the ^{3}ILCT* emission of **10** (10^{-5} M in CH_3CN) were obtained from the graph of I_o/I vs [Q] using $I_o/I = 1 + k_q\tau[Q]$, where I_o is the emission intensity of the ^{3}ILCT* in the absence of a quenching agent, I is the emission intensity of the ^{3}ILCT* at some quencher concentration [Q], and τ is the lifetime of **10** in the absence of a quenching agent. The uncertainties in k_q are reported at the 95% confidence limit and were propagated from the standard error of the slope and the estimated uncertainties in τ.

Electrochemical Experiments. Electrochemical experiments were conducted with a BAS CV50 in CV mode at a scan rate of 100 mV/s, using a glassy carbon working, a platinum auxiliary, and a Ag/AgCl reference electrode with [NBu_4][PF_6] (0.1 M) as the supporting electrolyte. Under these conditions, the ferrocene/ferrocenium couple (DMF) was found at 511 mV. Complex **6** was generated in the electrochemical cell by the addition of HBF_4·Et_2O to a solution of **10**. After the addition of HBF_4·Et_2O, a small sample was removed from the electrochemical cell and diluted, and the UV-vis spectra recorded to ensure that only the monoprotonated species was present. The oxidation and reduction potentials for **6** and **10** (Table 5) are reported relative to SCE using the ferrocene/ferrocenium couple to adjust the measured values.

Results and Discussion

Reactions of the group VIII transition metal bishydrosulfido complexes dppeM$(SH)_2$, where M = Ni, Pd, and Pt,[24] with either 1-(quinoxylin-2-yl)bromoethanone or 1-(quinoxylin-2-yl)bromopropanone[26] yield the corresponding quinoxalinium-substituted metallo-1,2-enedithiolate complexes, **4**−**7** (Scheme 1). Complexes **8**−**11** were isolated upon the addition of triethylamine and subsequent column chromatography. Complexes **4**−**7** were regenerated quantitatively by the addition of HBF_4·Et_2O to **8**−**11**, respectively. The synthetic details and the spectroscopic characterization of **4**−**11** have been described elsewhere.[24]

Electronic Transitions. In addition to the local electronic transitions associated with the quinoxaline moiety, **8**−**10** possessed an additional lower-lying electronic transition at 440 nm (22 700 cm^{-1}, CH_2Cl_2), assigned to a 1,2-enedithiolate $\pi \rightarrow$ quinoxaline π^* charge transfer transition (ILCT). This assignment was based upon the following three observations. First, the energy of the band decreased with solvent polarity (from 23 260 cm^{-1} in CCl_4 to 22 120 cm^{-1} in DMSO), supporting the charge transfer assignment. However, these

(25) Harriman, A. *J. Chem. Soc., Faraday Trans. 1* **1980**, *76*, 1978−85.

(26) Rowe, D. J.; Garner, C. D.; Joule, J. A. *J. Chem. Soc., Perkin Trans. 1* **1985**, 1907−10.

Table 1. Electronic Transitions of Complexes **4**−**11** Recorded in CH_2Cl_2

complex	M	R, R′	λ_{max} (ϵ), neutral	λ_{max} (ϵ), protonated
8, **4**	Ni	quin, H	240 (24900), 276 (20200), 302 (15900), 346 (6000),444 (5700)	240 (34800), 278 (25000), 372 (4300), 568 (11000)
9, **5**	Pd	quin, H	240 (21000), 281 (15500), 308 (11500), 342 (5200),443 (5300)	240 (25800), 282 (21200), 392 (4900), 564 (11700)
10, **6**	Pt	quin, H	244 (29900), 274 (26800), 306 (8400), 326 (9400),442 (6000)	248 (33700), 276 (24300), 396 (5600), 564 (11600)
11, **7**	Pt	quin, Me	248 (23500), 270 (25100), 310 (14600), 328 (13300), 464 (5300)	250 (32300), 270 (25100), 313 (12900), 428 (9800),605 (15900)

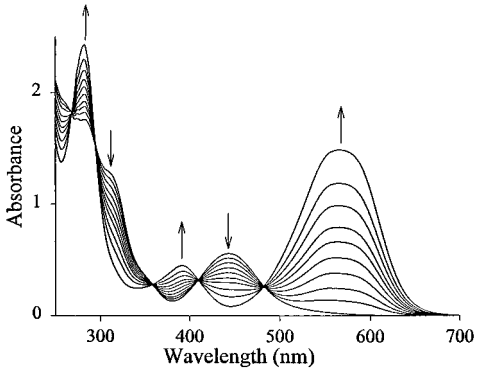

Figure 1. The titration of **9** with HBF_4 to generate **5** as monitored by UV-vis spectroscopy. The arrows denote the absorption decrease (↓) and increase (↑), respectively.

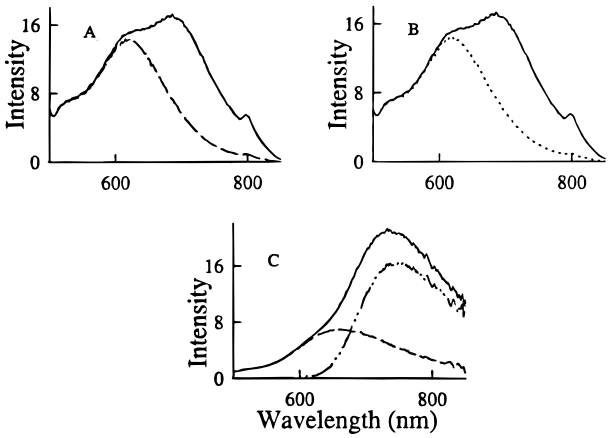

Figure 2. (A) The uncorrected emission spectra of **10** (CH_3CN) at 298 K: under nitrogen (solid line); in air (dashed line). (B) The uncorrected emission spectra of **10** (CH_3CN) at 298 K: under nitrogen (solid line); in the presence 1.5×10^{-3} M benzoic acid (dotted line). (C) Corrected emission spectra of **10** (CH_3CN) at 298 K: under nitrogen (solid line); in air (dashed line); the difference spectrum (dashed/dotted line).

spectral shifts did not correlate with the polarity constants E^*_{MLCT} and π^*.[27] Second, replacing H (**10**) with Me (**11**) and protonation of the quinoxaline (Table 1 and Figure 1) shifted this transition to the red (by 1140 and 5160 cm^{-1}, respectively). Taken together, these observations are consistent with an intraligand charge transfer transition. Third, the energy of this band was identical for the Ni, Pd, and Pt 1,2-enedithiolate complexes (Table 1), thus ruling out assignment of this band to a MLCT, LMCT, or d → d transition.[28−33]

Luminescence. Unlike the corresponding Ni and Pd complexes, **8** and **9**, aerated room temperature solutions of the Pt complexes **10** and **11** exhibited a single broad emission with no discernible vibronic structure. Following the removal of O_2, an additional, lower-energy band was observed (Figure 2). Emission intensities were linear with concentration, and the excitation spectra of both emission bands were identical to the absorption spectrum of **10** and **11**, respectively. The energies of both emission maxima were solvent sensitive and decreased with increasing solvent polarity, consistent with a polar excited state (Tables 2 and 3). Although the shifts in the emission maxima with solvent polarity were >3000 cm^{-1}, the solvent dependence did not fit the Lippert equation,[34−36] suggesting the presence of specific solvent effects not readily accommodated by this simple continuum solvent model.

The quantum yields for the low energy band of **10**, $^3\phi$, were slightly larger than those of the high-energy band, $^1\phi$, in all solvents (Table 2). The quantum yields were somewhat solvent sensitive, increasing by a factor of 10 from 0.002 in toluene to 0.02 in DMSO for the low-energy emission band and by a factor of 3 from 0.002 in toluene to 0.006 in DMSO for the high-energy emission band. The $^3\phi/^1\phi$ ratio also tracked with solvent polarity where $^3\phi/^1\phi = 1$ for toluene and $^3\phi/^1\phi = 3$ for DMSO. As can be seen from a comparison of Tables 2 and 3, the quantum yields for **11** were uniformly lower than those for **10**, but followed similar solvent polarity trends.

Luminescence lifetime measurements of deaerated solutions of **10** and **11** provided frequency plots that were best fit as a sum of two exponential decays with one very short-lived component (0.08−0.18 ns) and one very long-lived component (350−4700 ns) (Tables 2 and 3). The percentage of emission arising from each component was in agreement with the relative emission intensities of the two bands observed in the steady state measurements (prior to instrument correction). The addition of dioxygen largely eliminated the lower-energy, longer-lived component, leaving the higher-energy, shorter-lived component essentially unaffected. Mirroring the lower quantum yields, the lifetimes of both the long- and short-lived components of **11** were significantly reduced relative to those of **10**. Since the lifetime of the state associated with the low-energy emission of **11** was significantly shorter than that of **10**, it was not completely quenched in either air or dioxygen. Thus, a component with a shorter lifetime and a substantially reduced emission percentage was observed for **11** in both air and dioxygen (Table 3). While a similar component was observed in aerated solutions of **10**, in most solvents it accounted for less than 5% of the total emission (Table 2). From the solubilities of dioxygen in dimethyl sulfoxide, pyridine, and methylene chloride and the emission lifetimes of **11** (Table 3), the second-order rate constants for dioxygen quenching of the lower-energy emission of **11** were estimated to be near the diffusional limit ($\geq 3 \times 10^9$ M^{-1} s^{-1}) in these solvents.[37]

The radiative rate constants, $k_r = \phi/\tau$, calculated for the higher-energy band ($k_r \approx 3 \times 10^7$ s^{-1}) and the lower-energy

(27) Manuta, D. M.; Lees, A. J. *Inorg. Chem.* **1983**, *22*, 3825−28.
(28) Gray, H. B.; Ballhausen, C. J. *J. Am. Chem. Soc.* **1963**, *85*, 260−4.
(29) Shupack, S. I.; Billig, E. C.; Williams, R.; Gray, H. B. *J. Am. Chem. Soc.* **1964**, *86*, 4594−602.
(30) Werden, B. G.; Billig, E.; Gray, H. B. *Inorg. Chem.* **1966**, *5*, 78−81.
(31) Fackler, J. P.; Coucouvanis, D. J. *J. Am. Chem. Soc.* **1966**, *88*, 3913−20.
(32) Bowmaker, G. A.; Boyd, P. D. W.; Campbell, G. K. *Inorg. Chem.* **1983**, *22*, 1208−13.
(33) Vogler, A.; Kunkely, H.; Hlavatsch, J.; Merz, A. *Inorg. Chem.* **1984**, *23*, 506−9.
(34) Lippert, V. E. *Z. Electrochem.* **1957**, *61*, 962−75.
(35) Kawski, A. *Acta Phys. Pol.* **1966**, *29*, 507−18.
(36) Mataga, N.; Y., K.; Koizumi, M. *Bull. Chem. Soc. Jpn.* **1956**, *29*, 465−70.

Table 2. Solvent Dependence of the Luminescence Maxima, Quantum Yields, and Lifetimes of **10**

solvent	$^1\phi^a$	$^3\phi$	$^1\lambda^a$	$^3\lambda^a$	$^{air}\tau^b$	$^{Ar}\tau^b$
DMSO	0.006	0.02	660	748	0.15 (86), 288 (14)	0.15 (38), 4700 (62)
CH_3CN	0.005	0.01	653	748	0.16 (96)	0.16 (49), 3300 (51)
DMF	0.004	0.009	642	744		
acetone	0.004	0.01	626	733		
pyridine	0.005	0.01	632	719	0.18 (96)	0.18 (43), 3400 (57)
CH_2Cl_2	0.004	0.006	636	720	0.14 (89), 208 (11)	0.14 (48), 4100 (52)
$CHCl_3$	0.003	0.004	639	734		
THF	0.002	0.004	591	701	0.08 (95)	0.08 (63), 2200 (39)
dioxane	0.002	0.003	576	693		
toluene	0.002	0.002	540	655		

[a] Emission maximum in nanometers. [b] Lifetime in nanoseconds where the value in parentheses is the percentage (%) of emission attributed to that component.

Table 3. Solvent Dependence of the Luminescence Maxima, Quantum Yields, and Lifetimes of **11**

solvent	$^1\phi$	$^3\phi$	$^1\lambda^a$	$^3\lambda^a$	$^{O_2}\tau^b$	$^{air}\tau^b$	$^{Ar}\tau^b$
DMSO	0.0009	0.001	701	744	0.11 (90), 15 (10)	0.11 (83), 135 (17)	0.11 (45), 720 (55)
pyridine	0.0008	0.0008	691	738	0.11 (92), 15 (8)	0.11 (79), 100 (21)	0.11(48), 660 (52)
CH_2Cl_2	0.0006	0.0004	680	725	0.05 (92), 8.8 (8)	0.05 (77), 110 (23)	0.05 (60), 350 (40)

[a] Emission maximum in nanometers. [b] Lifetime in nanoseconds where the value in parentheses is the percentage (%) of emission attributed to that component.

band ($k_r \geq 3 \times 10^3$ s^{-1})[38] of **10** in acetonitrile, were consistent with these emissions originating from an intraligand charge transfer singlet state (^{1}ILCT*) and an intraligand charge transfer triplet state (^{3}ILCT*), respectively. The large nonradiative rate constant, $k_{nr} = (1/\tau) - k_r$, observed for the ^{1}ILCT* of **10** ($k_{nr} \approx 6 \times 10^9$ s^{-1}) likely arises from an increased rate of intersystem crossing resulting from enhanced spin-orbit coupling due to the presence of the Pt (internal heavy atom effect).[39] Similarly, the radiative ($k_r \geq 3 \times 10^3$ s^{-1}) and nonradiative rate ($k_{nr} \leq 3 \times 10^5$ s^{-1}) constants estimated for the ^{3}ILCT* were consistent with their enhancement by spin-orbit coupling.[38,39]

The radiative and nonradiative rate constants for the ^{1}ILCT* ($k_r \approx 8 \times 10^6$ s^{-1}, $k_{nr} \approx 9 \times 10^9$ s^{-1}) and for the ^{3}ILCT* ($k_r \geq 1 \times 10^3$ s^{-1}, $k_{nr} \leq 1 \times 10^6$ s^{-1}) of **11** are similar to those estimated for complex **10** and are consistent with the excited state assignments.

Ground state protonation of either **10** or **11** (yielding **6** and **7**, respectively) resulted in the loss of both emissions in the visible region. Whether these protonated complexes are emissive in solution at room temperature is currently unclear. If **6** or **7** had Stokes shifts similar to **10** and **11**, the emission bands would be outside the spectral range of our fluorimeter (≥850 nm) and thus undetectable. The related pyridinium complexes [(dppe)Pt{S_2C_2(2-pyridinium)(H)}][BF_4] and [(dppe)Pt{S_2C_2-(4-pyridinium)(H)}][BF_4] have recently been prepared.[24b] These protonated complexes are emissive, clearly demonstrating that protonation of the heterocycle does not necessarily lead to quenching of the ILCT* at room temperature.

Quenching of the ^{3}ILCT* by Electron Transfer.[40] In addition to its quenching by dioxygen, the ^{3}ILCT* was quenched by electron acceptors and donors having appropriate redox potentials. The thermodynamic driving force for excited state electron transfer in polar solvents was estimated from the relation

$$\Delta G_e = -E_{oo} + E_{ox} - E_{red} \quad (1)$$

where E_{oo} for the ^{3}ILCT* was approximated from its emission maximum (Table 2 and 3) and E_{ox} and E_{red} are the oxidation potential of the electron donor and the reduction potential of the electron acceptor (Table 4), respectively.[41] Reduction and oxidation potentials for *p*-dinitrobenzene (DNB), dicyanobenzene (DCB), *N*,*N*-dimethylaniline (DMA), and *N*,*N*,*N*′,*N*′-tetramethyl-*p*-phenylenediamine (TMPD) were obtained from the literature,[41−43] whereas oxidation and reduction potentials for **10** were obtained by cyclic voltametry in DMF. The thermodynamic driving forces calculated for the quenching of the ^{3}ILCT* by these donors and acceptors are collected in Table 4. As anticipated from the thermodynamic calculations, both the electron acceptor, DNB, and the electron donor, TMPD, efficiently quenched the ^{3}ILCT* emission with rate constants that were ≥10^9 (Table 4). The electron donor, DMA, and the acceptor, DCB, had no affect on the ^{3}ILCT* emission of **10** at concentrations ≤1 M. Assuming that a 10% reduction in steady state emission intensity should be easily observed, these results indicate that the rate of electron transfer between the ^{3}ILCT* and these compounds must be < 3.4×10^4 M^{-1} s^{-1}. These findings were in general agreement with the calculated thermodynamic driving forces that indicated electron transfer from the ^{3}ILCT* to DCB was endergonic and electron transfer from DMA to the ^{3}ILCT* was at best, only slightly exergonic.

Quenching of the ^{3}ILCT* by Weak Acids and Hydrogen Atom Donors. The nitrogens of the quinoxaline are expected to bear additional electron density in the ILCT* excited states. This should increase the basicity of the excited states relative to the ground state. Given the long lifetime of the ^{3}ILCT*, it should be readily quenched by concentrations of acids that are insufficient to protonate the ground state complex.[44] Because the ground state pK_a of **10** in acetonitrile is 11.9,[24] a 10^{-5} M solution of **10** was unaffected by the addition of 10^{-3} M benzoic acid (pK_a = 20.7).[45] However, this concentration

(37) Murov, S. L; Carmichael, I; Hug, G. L *Handbook of Photochemistry, 2nd ed.*; Marcel Dekker, Inc.: New York, 1993; pp 289−93.

(38) The use of $k_r = \phi/\tau$ to calculate the radiative rate constant for the ^{3}ILCT* assumes that intersystem crossing from the ^{1}ILCT* proceeds with 100% efficiency, which may not be an unreasonable approximation given the presence of the platinum. However, in the absence of information on triplet yields, the value reported for k_r is a lower bound while the k_{nr} is an upper bound.

(39) Birks, J. B. *Photophysics of Aromatic Molecules*; Wiley-Interscience: London, 1970; Vol. 6, pp 193−297.

(40) In all quenching studies due to the short lifetime of the ^{1}ILCT*, only quenching of the ^{3}ILCT* was observed.

(41) Kavarnos, G. J.; Turro, N. J. *Chem. Rev.* **1986**, *86*, 401−49.

(42) Bordwell, F. G.; Cheng, J.-P. *J. Am. Chem. Soc.* **1991**, *113*, 1736−43.

(43) Bordwell, F. G. *Acc. Chem. Res.* **1988**, *21*, 456−63.

Table 4. Thermodynamic and Kinetic Parameters Associated with Quenching of the ^{3}ILCT* of **10** in Acetonitrile

	E_{ox} (V)	E_{red} (V)	p$K_{a(q)}$	ΔG_e (eV)[a]	$\Delta G_{H^\bullet}$ (eV)[b]	ΔG_{H+} (eV)[c]	k_q($\times 10^9$ M^{-1}s^{-1})[d]
complex **10**	+0.54[e]	−0.84[e]					
complex **6**	+0.59[e]	−0.59[e]	11.9				
dinitrobenzene		−0.69[f]		−0.43			2.9 ± 0.7
dicyanobenzene		−1.64[f]		+0.52			<0.00003
N,*N*-dimethylaniline	+0.81[f]			−0.01			<0.00003
N,*N*,*N*′,*N*′-tetramethyl-*p*-phenylenediamine	−0.16[f]			−0.98			5.0 ± 1
pyridinium			12.3[h]			−0.57	25 ± 6
diammoniopropane			15.0[h]			−0.41	19 ± 5
salicylic acid			16.7[h]			−0.31	12 ± 3
triethylammonium			18.5[h]		+0.10	−0.21	6.0 ± 1
triethylamine	+0.76[f]						
benzoic acid			20.7[h]			−0.08	3.0 ± 0.7
o-nitrophenol		-0.94[e]	22.0[h]	−0.18		0.00	2.0 ± 0.5
phenol	+2.10[g]		26.6[h]	+1.28	−0.38	+0.27	0.40 ± 0.09
phenoxide	−0.18[g]						
p-methoxyphenol	+1.10[g]		27.7[i]	+0.38	−0.45	+0.34	0.98 ± 0.2
p-methoxyphenoxide	−0.31[g]						
p-dihydroquinone	+1.57[g]		28.4[i]	+0.67	−0.67	+0.38	2.7 ± 0.6
[*p*-dihydroquinone]$^-$	−0.57[g]						
methanol			≥32[j]			+0.59	0.036 ± 0.0001

[a] Calculated using eq 1. [b] Calculated using eq 3. [c] Estimated assuming an excited state pK_a of 22 using $\Delta G_{H^+} = -0.059(22 - pK_{a(q)})$. [d] The uncertainties are reported at the 95% confidence limits. [e] Values measured in this work and reported versus SCE. [f] Values reported versus SCE.[41] [g] Values adjusted to a SCE reference electrode using the reported internal ferrocene/ferrocinium couples.[42] [h] pK_a values reported in acetonitrile.[45] [i] The pK_a was estimated by subtracting 8.6 units from the pK_a in DMSO (8.6 units is the difference in the pK_a of phenol in DMSO and acetonitrile).[42,45] [j] Assumed to be greater than or equal to the value reported for MeOH in DMSO.[43]

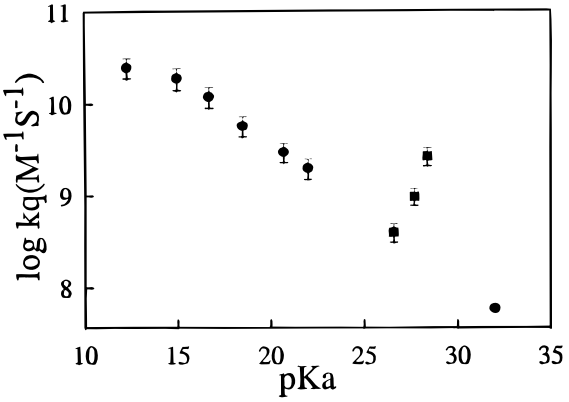

Figure 3. Dependence of k_q (log scale) versus pK_a of the quenching agent. Those agents considered proton donors are indicated by ●, and those agents considered hydrogen atom donors are indicated by ■. Error bars represent the 95% confidence limits of k_q. See Table 4 for the tabular data.

of benzoic acid was sufficient to completely quench the ^{3}ILCT* emission. Due to its short lifetime, the emission from the ^{1}ILCT* was unaffected (Figure 2, insert B). Stern−Volmer plots for the quenching of the ^{3}ILCT* emission of **10** by a range of acids in acetonitrile gave k_q values that decrease with increasing pK_a of the quencher. These values ranged from 2.5 $\times$ 10^{10} M^{-1} s^{-1} for pyridinium to 3.6 $\times$ 10^7 M^{-1} s^{-1} for methanol (Table 4 and Figure 3). With the possible exception of phenol, *p*-methoxyphenol, dihydroquinone, and nitrophenol, thermodynamic calculations indicated that quenching by these acids could not be attributed to either electron or hydrogen atom transfer (Table 4).

The high pK_a values of the acids that quenched the ^{3}ILCT* provided clear evidence that this state was significantly more basic than the ground state. Unfortunately, because luminescence from the protonated complexes **6** and **7** could not be observed, it was unclear whether equilibrium was established in the excited state proton transfer. Thus, these experiments did not allow a pK_a for the ^{3}ILCT* to be determined using the classical Förster analysis (eq 2).[44,46]

$$pK_a^* = pK_a + (0.625/T)(\nu_B - \nu_{BH^+}) \qquad (2)$$

However, the shifts in absorption energy observed upon protonation of the ground state complex **10** can provide a bound on this value. In the analysis, K_a and K_a* are the ground and excited state equilibrium constants, T is the temperature, and ν_{HB^+} and ν_B are the ^{1}ILCT transition energies (in cm^{-1}) of the protonated (HB^+) and neutral (B) complexes, respectively. Using the absorption maxima of the protonated and deprotonated forms of **10** to estimate the ν values (Table 1) along with the measured value of the ground state pK_a in acetonitrile of 11.9,[24] values on the order of 22−23 were obtained. Assuming that the shift in triplet energy between protonated and deprotonated forms is approximately equal to that for the singlet and that equilibration takes place in the excited state, a pK_a* of 22−23 in acetonitrile would be expected for the ^{3}ILCT*. This result was consistent with the dependence of k_q on pK_a (Figure 3), where k_q drops from the diffusional limit as the thermodynamic driving force for proton transfer falls.[47] Given these findings, the thermodynamic driving forces for the proton transfer reactions (Table 4) were estimated assuming a pK_a* of 22 and the literature pK_a values for the quenching acids in acetonitrile.

While proton transfer from *o*-nitrophenol to the ^{3}ILCT* was estimated to be thermoneutral, electron transfer from the ^{3}ILCT* to *o*-nitrophenol should be slightly exergonic. The k_q associated with *o*-nitrophenol was consistent with the relationship exhibited by the other acid quenchers (Figure 3), but electron transfer

(44) (a) Vos, G. J. *Polyhedron* **1992**, *11*, 2285−99. (b) Nazeeruddin, M. K.; Kalyanasundaram, K. *Inorg. Chem.* **1989**, *28*, 4251−9. (c) Davila, J.; Bignozzi, C. A.; Scandola, F. *J. Phys. Chem.* **1988**, *93*, 1373−80. (d) Giordano, P. J.; Bock, R.; Wrighton, M. S. *J. Am. Chem. Soc.* **1978**, *100*, 6960−65. (e) Shinozaki, K.; Ohno, O.; Kaizu, Y.; Kobayashi, H.; Sumitani, M.; Yoshihara, K. *Inorg. Chem.* **1989**, *28*, 3680−3. (f) Ireland, J. F.; Wyatt, P. A. H. *Advances in Physical Organic Chemistry*; Gold, V., Bethell, D., Eds. Academic Press: New York, 1976; *12*, 131−221. (g) Kosower, E. M.; Huppert, D. *Ann. Rev. Phys. Chem.* **1986**, *37*, 127−56.
(45) Coetzee, J. F.; Padmanabhan, G. R. *J. Am. Chem. Soc.* **1965**, *87*, 5005−10.
(46) Förster, T. *Z. Electrochem.* **1950**, *54*, 531.
(47) Rehm, D.; Weller, A. *Isr. J. Chem.* **1970**, *8*, 259−71.
(48) Zuleta, J. A.; Burberry, M. S.; Eisenberg, R. *Coord. Chem. Rev.* **1990**, *97*, 47−64.

cannot be excluded as a mechanism for its quenching of the ^{3}ILCT*.

Because the ^{3}ILCT* was both a better electron and proton acceptor than the ground state, it should serve as a better hydrogen atom acceptor than **10**. The thermodynamic driving forces for hydrogen atom donation to the ^{3}ILCT*were estimated from the equation

$$\Delta G_{H\bullet} = -E_{oo} + E_{ox} - E_{red} - 0.059(pK_{a(\mathbf{6})} - pK_{a(q)}) \quad (3)$$

where E_{ox} and E_{red} were the oxidation potential of the conjugate base of the quencher and the reduction potential of **6**, respectively.[41] The pK_a of **6** (p$K_{a(\mathbf{6})}$) was determined to be 11.9,[24] whereas the pK_a values of the quenchers (p$K_{a(q)}$) were obtained from the literature.[41−43] Of all of the acids examined, only triethylammonium, phenol, *p*-methoxyphenol, and *p*-dihydroquinone had $\Delta G_{H\bullet}$ values that were estimated to be either negative or only slightly positive. The k_q values for *p*-methoxyphenol and *p*-dihydroquinone were larger than that for phenol, even though they were less acidic. Furthermore, the k_q values of these two acids clearly deviated from the relationship between k_q and pK_a established for the other acids (Figure 3 and Table 4). These results support the notion that hydrogen atom transfer is the dominant mechanism by which *p*-methoxyphenol and *p*-dihydroquinone quench the ^{3}ILCT*.

Because the k_q for triethylammonium was quite large and its $\Delta G_{H\bullet}$ was slightly positive (Table 4), proton transfer seems a much more plausible mechanism for its quenching of the ^{3}ILCT* emission. If triethylammonium was a hydrogen atom donor to the ^{3}ILCT*, the estimated $\Delta G_{H\bullet}$ suggests that it would be much less effective as a quenching agent. Thus, its k_q would be expected to be below that of phenol and well below that of *p*-methoxyphenol and p-dihydroquinone. The mechanism by which phenol quenches the ^{3}ILCT* emission is unclear, since the observed value for k_q (Table 4) could be interpreted as due to either a proton or a hydrogen atom transfer reaction.

Conclusion

Metallo-1,2-enedithiolates and in particular, heterocyclic-substituted 1,2-enedithiolates, are an interesting new class of solution lumiphores. A novel synthetic route to these complexes is amenable to the incorporation of a range of appended groups and ancillary ligands and is being fully developed in this regard.[24]

The lowest-energy electronic transition in the quinoxaline substituted 1,2-enedithiolate complexes was acid sensitive and was assigned to an intraligand charge transfer transition (ILCT). The platinum complexes (dppe)Pt{S_2C_2(2-quinoxaline)(R)} have two emissive states that were assigned to an ^{1}ILCT* and an ^{3}ILCT* on the basis of their energies and lifetimes. Previous studies suggested that phosphine-substituted complexes, such as (dppe)Pt($S_2C_2R_2$) where R = C(O)Me, and CN,[48] were luminescent only at low temperatures in a frozen matrix. However, the room temperature luminescence of (dppe)Pt{S_2C_2-(2-quinoxaline)(R)} as well as that of [(dppe)Pt{S_2C_2(2-pyridinium)(H)}][BF_4],[24b] [(dppe)Pt{S_2C_2(4-pyridinium)(H)}][BF_4],[24b] and [(dppe)Pt{S_2C_2(2-pyrazinium)(H)}][BF_4][24b] suggest that a range of heterocyclic-substituted metallo-1,2-enedithiolates of platinum, including those complexes containing phosphine ligands, should be emissive in solution.

The charge transfer nature of the excited states, accompanied by the availability of the heterocyclic nitrogens, leads to a substantial increase in the basicity of the appended heterocycle. While an increase in the basicity of the excited states of inorganic complexes has been observed in past studies,[44] this work has demonstrated that the rate of the excited state reaction depends on the thermodynamic driving force for the proton transfer and hence on the pK_a of the quenching acid. Deviations from this correlation for some compounds provided evidence that hydrogen atom transfer was the dominant mechanism of ^{3}ILCT* quenching.

Our data indicate that the ^{3}ILCT* of the quinoxaline-substituted complexes can undergo a diverse suite of excited state reactions including electron, proton, and hydrogen atom transfers. These results bode well for the rational construction of other 1,2-enedithiolate complexes that have been "tuned" for a particular type of excited state reaction through careful selection of the heterocyclic moiety.

Acknowledgment. We are indebted to the American Chemical Society, Petroleum Research Fund (grant no. 28499-G3), the Exxon Education Foundation, and the Office of the Naval Research (N00014-95-10201) for supporting this work.

Supporting Information Available: Experimental details and spectroscopic characterization for **4**−**11** and X-ray data for **5** and **8** (23 pages). See any current masthead page for ordering and Internet access instructions.

JA9626998